Food Research International 139 (2021) 109973

Contents lists available at ScienceDirect

Food Research International

journal homepage: www.elsevier.com/locate/foodres

Incorporating strain variability in the design of heat treatments: A stochastic approach and a kinetic approach

Marcel H. Zwietering, Alberto Garre, Heidy M.W. den Besten *

Food Microbiology, Wageningen University, PO Box 17, 6700 AA Wageningen, the Netherlands

ARTICLE INFO

Keywords:
Thermal processing
Inactivation
Monte Carlo simulation
Biological variation
Risk assessment
Pasteurization
Sterilization

ABSTRACT

For the design of thermal processes, the decimal reduction times (*D*-values) of target organisms can be used. However, many factors influence the *D*-value, like inherent organism's characteristics (strain variability), the effect of the history of the cells, as well as product factors and process factors. Strain variability is a very large contributor to the overall variation of the *D*-value. Hence, the overall reduction of microbial contaminants by a heat treatment is a combination of the occurrence of a strain with a certain heat resistance and its reduction given the prevailing conditions. This reduction can be determined using two approaches: a kinetic analysis based on integral equations or a stochastic approach based on Monte Carlo analysis. In this article, these two approaches are compared using as case studies the inactivation of two microorganisms: *Listeria monocytogenes* in a pasteurization process and the sporeformer *Geobacillus stearothermophilus* in a UHT process. Both approaches resulted in similar conclusions, highlighting that the strains with the highest heat resistance are determinant for the overall inactivation, even if the probability of cells having such extreme heat resistance is very low.

1. Introduction

The concepts of appropriate level of protection (ALOP) and food safety objective (FSO) have been set up to make food safety control transparent along the food chain. They enable the definition of quantitative targets for public health protection and for maximum tolerable contamination levels at different steps of the food production chain (ICMSF, 2018). To achieve an appropriate level of protection for a specific pathogen, this public health objective can be translated into a maximum tolerable concentration of the hazard in a food at the moment of consumption, the so-called FSO. When an FSO has been defined, the performance criteria (PC) can be set at the various food production steps using the ICMSF equation:

$$H_0 + \Sigma I - \Sigma R \leq \text{FSO} \quad (1)$$

with H_0 the initial level of the pathogenic contaminant, ΣI the sum of all increases of the hazard in the chain (due to growth and recontamination) and ΣR the sum of all reductions of the hazard. FSO, H_0, R and I are all expressed in $\log_{10}$ units.

If we have a process without growth and recontamination (i.e. $\Sigma I = 0$) this results in:

$$H_0 - \Sigma R \leq \text{FSO} \quad (2)$$

with the FSO determined by the initial level, H_0, and the sum of the reductions. The reduction of the pathogen by, for example, a heat treatment can be determined using quantitative microbiology models (McMeekin et al., 2002). Users of quantitative microbiology request accurate models to predict behavior of microorganisms in food products. It should however be realized that exact models do not exist, since reality is very variable. Also, both the initial contamination level and the reduction will not be fixed values but be variable due to many different aspects (Zwietering, 2015).

For the design of heat treatments often the *D*, *z*-concept is used to determine a target inactivation. The *D*-value is the decimal reduction time, which is the time it takes for 1 $\log_{10}$ (i.e. factor 10) reduction during an isothermal treatment. The *z*-value is the temperature increase needed to decrease the *D*-value by a factor of 10. In this paper we will focus on the variability in microbial reduction during a heat treatment. This variability in reduction is partly determined by the processing variables temperature and time, but will also depend on the product characteristic (e.g. pH and a_w) and variability therein, matrix effects, the specific strain of the organism, and the physiological state of the cells to be inactivated. In meta-analyses carried out for several pathogenic and spoilage organisms (Den Besten, Wells-Bennik, & Zwietering, 2018) it was found that the difference in the *D*-value can span up to two $\log_{10}$

* Corresponding author.
E-mail address: heidy.denbesten@wur.nl (H.M.W. den Besten).

https://doi.org/10.1016/j.foodres.2020.109973
Received 29 February 2020; Received in revised form 7 September 2020; Accepted 28 November 2020
Available online 8 December 2020

difference due to various effects, including but not limited to bacterial strain, product and history effects. It was concluded that variability between different strains is a major contributor to the overall variation and can result in more than a 1 $\log_{10}$ difference in the D-value of different strains. This implies that when some strains of the organism are inactivated by a heat treatment for a specific time and temperature regime by 10 $\log_{10}$ (i.e. factor 10^{10}, so virtually fully inactivated), others are only inactivated by 1 $\log_{10}$ (resulting in 10% survival). Although the chance of finding an extremely heat resistant strain is very low, these strains do have a much higher survival and determine the overall survival of a mixed population of strains. Therefore, strain variability can potentially be very relevant for the efficacy of the inactivation treatment. This was demonstrated using a kinetic approach for describing the effect of pasteurization on reduction of *Listeria monocytogenes* (Den Besten et al., 2018). This approach is further explored in this paper by comparing this kinetic analysis with a stochastic calculation to demonstrate how these different approaches can complement each other. Furthermore, sensitivity analyses are carried out to compare the impact of different influencing factors (time, temperature, the z-value, the mean of the $\log_{10}D$-value and its standard deviation) on various outcomes like the $\log_{10}$ inactivation but also the arithmetic number of the survivors (and the reduction then based on this arithmetic number of survivors). The impact of strain variability on achieved reduction of *Listeria monocytogenes* when performing a pasteurization treatment is also compared for an ultra-high temperature treatment that aimed to inactivate spores of *Geobacillus stearothermophilus*.

2. Materials and methods

2.1. Heat resistance of Listeria monocytogenes and Geobacillus stearothermophilus

Aryani et al. (2015) quantified the strain variability in heat resistance of *L. monocytogenes* by determining the heat resistance of 20 strains that were isolated from various sources. The overall z-value based on the D-values determined at 55 °C, 60 °C, 65 °C and 70 °C was 5.22 °C (Den Besten et al., 2018). Den Besten et al. (2018) reported the mean and standard deviation of $\log_{10}D_{72}$ based on these 20 strains assuming that the $\log_{10}D_{72}$ is normally distributed with mean of − 0.343 $\log_{10}$(s) and standard deviation of 0.226 $\log_{10}$(s). Wells-Bennik et al. (2019) followed a similar approach as Aryani et al. (2015) to quantify strain variability in heat resistance of *G. stearothermophilus* using spores of 18 different strains. The D-values were determined at 125 °C and 130 °C and resulted in an overall z-value of 11.1 °C. The mean heat resistance expressed in $\log_{10}D_{140}$ ($\log_{10}$(s)) was 0.00385 with a standard deviation of 0.171.

2.2. Determination of overall inactivation using a kinetic approach

The reduction or $\log_{10}$ inactivation, $R = -\log_{10}(N_t/N_0) = -(\log_{10}N_t - \log_{10}N_0)$ in a deterministic case in an isothermal case following log-linear inactivation, can be described by:

$$R = \log_{10}\text{inactivation} = -\log_{10}\left(\frac{N_t}{N_0}\right) = \frac{t}{D} = \frac{t}{10^{\log_{10}D}} \quad (3)$$

$$\frac{N_t}{N_0} = 10^{-\frac{t}{D}} = 10^{-\frac{t}{10^{\log_{10}D}}} \quad (4)$$

With N_t the number and $\frac{N_t}{N_0}$ the arithmetic fraction of survivors. The D-value is however not a constant value but varies because not all strains have the same thermal resistance. It can be assumed that the $\log_{10}D$-value can be described by a normal distribution, meaning that D is log-normally distributed (Aryani et al., 2015). In Den Besten et al. (2018) an integral equation was derived to determine the integrated lethal effect for a population of strains of which the D-value is log-normally distributed:

$$\frac{N_t}{N_0} = \int_{-\infty}^{\infty} f(u)10^{-\frac{t}{10^{\log_{10}D+\sigma u}}}du \quad (5)$$

With f the probability density function of a normal distribution with expected value μ and standard deviation σ. The variable u is a dummy variable for integration.

On $\log_{10}$-scale this results in:

$$\log_{10}\left(\frac{N_t}{N_0}\right) = \log_{10}\int_{-\infty}^{\infty} f(u)10^{-\frac{t}{10^{\log_{10}D+\sigma u}}}du \quad (6)$$

In this equation the lethal effect for a specific D-value is combined with the probability that such a heat resistant strain would be present. This equation can be solved numerically to determine the overall lethal effect of a specific process.

$$\log_{10}\left(\frac{N_t}{N_0}\right) = \log_{10}\frac{1}{\sqrt{2\pi}}\int_{-\infty}^{\infty}\exp\left(-\frac{u^2}{2}\right)10^{-\frac{t}{10^{\log_{10}D+\sigma u}}}du \quad (7)$$

This numerical integration was performed in MS Excel 2013®. The integration step for u was small (i.e. 0.01) to make the solution sufficiently stable.

2.3. Determination of overall inactivation using a Monte Carlo approach

The overall inactivation was also determined using Monte Carlo simulations that were also performed in MS Excel 2013® and verified using @RISK®. The number of iterations was 1,000,000 to come to a stable outcome.

2.4. Sensitivity analyses

For a given fixed D-value the reduction R as function of heating time would be expected to be linear:

$$R = \log_{10}\text{inactivation} = \frac{t}{10^{\log_{10}D}} = t\cdot 10^{-\log_{10}D} \quad (8)$$

The effect of temperature on the $\log_{10}$ of the reduction would also be expected to be linear:

$$\log_{10}R = \log_{10}t - \log_{10}D = \log_{10}t - \log_{10}D_{\text{ref}} + \frac{T - T_{\text{ref}}}{z} \quad (9)$$

With D_{ref} the D-value at the reference temperature ($T_{ref} = 72$ °C), and z the z-value.

The sensitivity for R has been calculated analytically in Appendix A for several variables, taking into account that the $\log_{10}D$-value is not fixed but has a variability. The sensitivity analysis was also done with the overall number of survivors on arithmetic scale as output, taking the variability in $\log_{10}D$-value into account, and then the $\log_{10}$ fraction of the survivors was calculated, $\log_{10}\left(\frac{N_t}{N_0}\right)$. Note, that this latter value is not equal to the average $\log_{10}$ inactivation, since first the average is determined and afterwards the logarithm, and this gives another outcome than averaging the $\log_{10}$-values.

Sensitivity analyses were performed in MS Excel 2013® and calculations were verified in R. The impact of variation in different variables on achieved reduction was tested, namely, variation in heating time, temperature, the z-value and the standard deviation of $\log_{10}D$. When testing one variable, the other variables were fixed at the reference condition, which was heat treatment for 15 s at 72 °C, z-value of 5.22 °C, and standard deviation of the $\log_{10}D_{72}$ equals 0.226 $\log_{10}$(s).

3. Results

3.1. Overall inactivation using a kinetic approach

Generally, it is assumed that a process of 15 s at 72 °C gives a

sufficient reduction of *L. monocytogenes* in milk (Bean et al., 2012). Strain variability in heat resistance is an important factor that determines the efficacy of a heat treatment to reduce all contaminants to an acceptable level. Aryani et al. (2015) quantified the strain variability in heat resistance and expressed the strain variability in the standard deviation of the $\log_{10}D$-value, assuming a normal distribution of the $\log_{10}D$-value, with a mean $\log_{10}D_{72}$-value and standard deviation of −0.343 $\log_{10}$(s) and 0.226 $\log_{10}$(s), respectively (Fig. 1, blue line). The following up study of Den Besten et al. (2018) calculated the achieved overall reduction taking into account this strain variability. This calculation was performed by a numerical integration (Equation (5)), combining the probability of a certain $\log_{10}D$-value and the achieved reduction, taking into account the whole probability distribution of $\log_{10}D$-values (Fig. 1, yellow line).

Based on an average $\log_{10}D$-value and corresponding D-value ($10^{-0.343}$ s), 33.1 $\log_{10}$ inactivation would be achieved with a heat treatment for 15 s at 72 °C. However, when taking into account the strain variability in $\log_{10}D$-values and the probability to have these cells with this heat resistance, and thus integrating the effect of strain variability, a 7.8 $\log_{10}$ inactivation would be achieved. This value of 7.8 $\log_{10}$ inactivation is much lower than expected based on the average $\log_{10}D$-value, and is equivalent to the number of reductions calculated when assuming that every heat-treated cell had a D-value corresponding to the 99.7th percentile of the $\log_{10}D$-value distribution. Likewise, the 97.5th percentile would give 11.9 $\log_{10}$ inactivation and the 99th percentile 9.8 $\log_{10}$.

3.2. Overall inactivation using a Monte Carlo approach

Alternatively, the analysis to determine the overall reduction can be performed by a Monte Carlo analysis (Balsa-Canto, Alonso, & Banga, 2008). In this approach multiple random samples or draws are taken from the normal distribution of the $\log_{10}D$-value (Fig. 2). Subsequently, the distribution of D-values can be estimated by taking the exponent with base 10 of the sampled $\log_{10}D$-values (Fig. 3). The D-values that are calculated for the two extreme points that were highlighted in Fig. 2 (colored green: $\log_{10}D_{72}$ is 0.313 $\log_{10}$(s); and colored orange: $\log_{10}D_{72}$ is 0.325 $\log_{10}$(s)) are also shown in Fig. 3. It is obvious from these two data points that the inverse $\log_{10}$-transformation makes these points even more extreme.

For each of the simulated D_{72}-values the reduction can be determined for a heat treatment of 15 s at 72 °C with 15/D (Fig. 4). The extreme points are again indicated using the same color code as for the previous figures. This figure illustrates that the majority (more than 80%) of the draws or iterations give 20–100 $\log_{10}$ inactivation, which can be considered as absolute inactivation, and these draws contribute only very limited to the overall achieved level of reduction. However, some random draws result in much lower reductions. It should be realized that a treatment causing 4 $\log_{10}$ inactivation differs from a treatment with 10 $\log_{10}$ inactivation by a factor of one million cells, so these few draws have a very relevant impact on the overall achieved reduction. For all random draws, the number of survivors can be

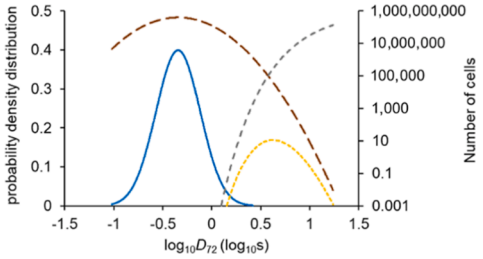

Fig. 1. Probability density distribution of $\log_{10}D_{72}$-values following a normal distribution (linear scale) (blue line), the number of cells having these $\log_{10}D_{72}$-values assuming $N_0 = 10^9$ cells ($\log_{10}$ scale, right) (brown line, long-size dashes, this is the blue line (linear scale, left) multiplied with 10^9), the number of cells from 10^9 cells that would survive a 15 s heat treatment given such a D_{72}-value ($\log_{10}$ scale, right) (grey line, medium-size dashes, this is $10^{9}*10^{-15/D}$), and the integrated number of surviving cells based on the log-normal distribution of D_{72}-values ($\log_{10}$ scale, right) (yellow line, small-size dashes, the combination of the brown long-size dashed line and the grey small-dashed line), thus combining the probability and the inactivation effect (adapted from Den Besten et al., 2018). (For interpretation of the references to color in this figure legend, the reader is referred to the web version of this article.)

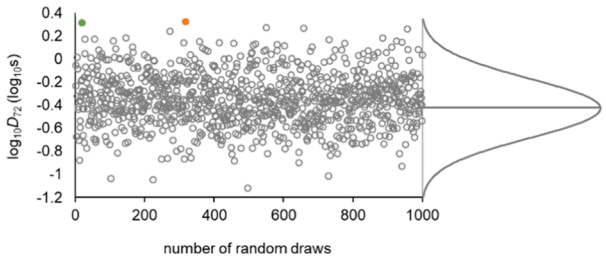

Fig. 2. 1000 random draws from a normal distribution of $\log_{10}D_{72}$-values (in $\log_{10}$(s)), with a distribution mean $\log_{10}D_{72}$ − 0.343 $\log_{10}$(s) and standard deviation 0.226 $\log_{10}$(s), and the density distribution of $\log_{10}D_{72}$ (grey line) of the random draws. Two high $\log_{10}D_{72}$-values are indicated in orange and green. (For interpretation of the references to color in this figure legend, the reader is referred to the web version of this article.)

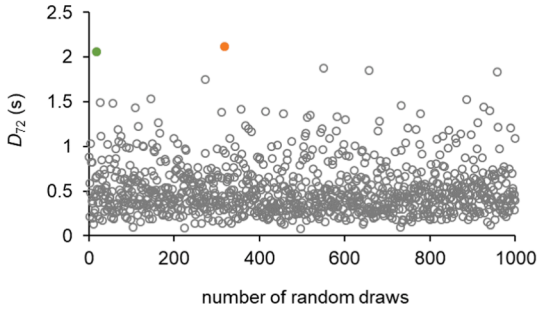

Fig. 3. 1000 random draws for the D_{72}-value from a log-normal distribution of D_{72}-values (in s), having as mean $\log_{10}D_{72}$ − 0.343 $\log_{10}$(s) and standard deviation 0.226 $\log_{10}$(s). The same high values in green and orange are indicated, but now on linear scale. (For interpretation of the references to color in this figure legend, the reader is referred to the web version of this article.)

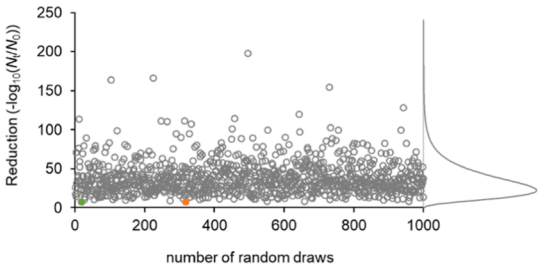

Fig. 4. 1000 values for the reduction (R) of cells ($-\log_{10}(N_t/N_0)$) when heat treated at 72 °C for 15 s, based on random draws from a log-normal distribution of D_{72}-values (in s), having as mean $\log_{10}D_{72}$ − 0.343 $\log_{10}$(s) and standard deviation 0.226 $\log_{10}$(s), and the density function of R (grey line) of the random draws. This density function of R is skewed, but when the R-values are $\log_{10}$-transformed, then the density function becomes normal-shaped. The lower R-values of the distribution are most relevant and determine the number of survivors. The green and orange points are now on the low site of the graph (small reduction). The median is at 33 $\log_{10}$ inactivation. (For interpretation of the references to color in this figure legend, the reader is referred to the web version of this article.)

calculated assuming an initial population of 10^5 cells (chosen as illustration for a population in a large quantity of food for example a bulk tank of milk) for each of the draws. To show more extreme values 10,000 random draws are represented in Fig. 5, with again the two extremes from the first 1000 random draws indicated using the same color code as above. The sum of the survivors of all draws is then the number of survivors from 10^9 cells, being 10^5 cells in each of the 10,000 random draws. This means that there are 10,000 draws of *D*-values, simulating variability in *D*-values, and that for each typical *D*-value there are initially 10^5 cells present with this characteristic. By summating the surviving cells from the 10,000 random draws, the total number of survivors from 10^9 cells can be determined. This resulted in about 25 cells surviving from 100,000 cells in 10,000 iterations, which is 25 cells from 10^9 cells and this represents a fraction of surviving cells of $2.5{\cdot}10^{-8}$, indicating 7.6 $\log_{10}$ inactivation. When these 10,000 iterations were repeated the outcome differed from 25 cells, e.g. the outcome was between 0.6 and 335 cells. The reason for that is the use of a numerical method whose truncation error depends on the number of iterations. Using 10,000 iterations the relative prediction error is rather high (25 and also values between 0.6 and 335 were output values), so 10,000 iterations was clearly not yet sufficient to give a stable estimate. Therefore, the number of iterations were increased to 1,000,000 draws, calculating an average reduction of 7.8 $\log_{10}$ that remained stable when the calculations were repeated (meaning that 15 cells survived from 10^9 cells).

This overall reduction based on this MC analysis is equal to the previously performed kinetic numerical analysis that also showed a 7.8 $\log_{10}$ reduction (Den Besten et al., 2018) and confirms that both approaches - a kinetic analysis and a Monte Carlo simulation - result in an equal outcome.

These simulations were performed using the native functions included in MS Excel 2013®, but can also be reproduced in @RISK. Excel has as advantage that intermediate results and all specific simulation results are visible and can be investigated, but @RISK can more easily perform large number of random draws, i.e. iterations, and statistical analysis of the output is more easily represented. Therefore, the calculations were also reproduced in @RISK using the same simulation settings (parameter values and number of iterations).

In Table 1 it can be seen that, on average, there is a 37.8 $\log_{10}$ inactivation, while the median is 33.0 $\log_{10}$ inactivation. This median value of the reduction (in $\log_{10}$) corresponds to the reduction calculated using the mean (and the median) value of the $\log_{10}D_{72}$-value distribution ($R = 15/10^{-0.343} = 15/0.4539 = 33.04$ $\log_{10}$ inactivation). The reduction distribution is not symmetrical (see Fig. 4 and Appendix B) and the average reduction is higher (37.8 $\log_{10}$). Although the distribution of $\log_{10}D$-value is symmetrical, due to all calculations (exponentiation Eq. (3)) the distribution of the reduction becomes skewed.

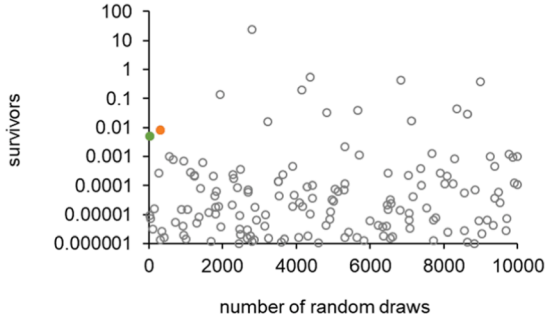

Fig. 5. Number of survivors from an initial total population of 10^9 cells that are heat treated at 72 °C for 15 s. Survivors are calculated for each of the 10,000 random draws, randomly taken from the log-normal distribution of D_{72}-values (in s), having as mean $\log_{10}D_{72}$ − 0.343 $\log_{10}$(s) and standard deviation 0.226 $\log_{10}$(s), with each draw representing 10^5 cells. Only those iterations with a number of survivors higher than 0.000001 cells is shown (most of the 10,000 points were lower; in this simulation 153 of the 10,000 points were above 0.000001, on average this was 172 out of 10,000).

Table 1
Results of a Monte-Carlo simulation in @RISK for the $\log_{10}$ inactivation of a heating process of 15 s at 72 °C, for a log-normally distributed *D*-value (in s), having as mean $\log_{10}D_{72}$ − 0.343 $\log_{10}$(s) and as standard deviation 0.226 $\log_{10}$(s).

	R (-$\log_{10}(N_t/N_0)$)	fraction survivors (N_t/N_0)	$\log_{10}$ fraction survivors ($\log_{10}(N_t/N_0)$)
Mode	25.34		
Median	33.04	$9.039{\cdot}10^{-34}$	−33.04
Average	37.84	$1.582{\cdot}10^{-8}$	−7.80
5th percentile	14.04		
1st percentile	9.85		

Due to the right-hand tail, the average $\log_{10}$ inactivation is higher than the median. The 1st, 5th, 95th and 99th percentiles are exactly what can be expected from the distribution of *D*-values (the locations of the percentiles do not change by exponentiating the value). However, from the point of view of the effectiveness of the inactivation treatment, the most relevant values are those where the microbial reduction is small. We can see a large difference between the 5th percentile (14.0 $\log_{10}$ inactivation) and the 1st percentile (9.9 $\log_{10}$ inactivation) (these correspond to the 95th and 99th percentiles of the *D*-values): a difference in the number of cells inactivated by a factor of 10,000 (4 $\log_{10}$). And there are some simulations where the number of reductions is even lower. To investigate the level of the survivors we have to investigate the arithmetic values; i.e. not the mean $\log_{10}$ inactivation but the overall fraction of survivors. The overall surviving fraction is $1.58{\cdot}10^{-8}$, that corresponds to 7.8 $\log_{10}$ inactivation. This is the $\log_{10}$ of the overall surviving fraction and that is different from the mean of the distribution of $\log_{10}$ of the survivors. This 7.8 $\log_{10}$ inactivation is a value lower than the 1st percentile of the $\log_{10}$ inactivation distribution. The median is again located at $9.0 \cdot 10^{-34}$ fraction survivors, which is 33.0 $\log_{10}$ inactivation, and this equals the result at the average $\log_{10}D$-value. Therefore, those cells in the microbial population with extreme *D*-values are the ones that determine the final number of survivors.

3.3. Sensitivity analysis

The sensitivity analysis was done with the arithmetic number of survivors, taking the variability in $\log_{10}D$-value into account and then the $\log_{10}$ fraction of the survivors was calculated, $\log_{10}\left(\frac{N_t}{N_0}\right)$. This cannot be solved analytically and therefore the numeric approach was used. First, the effect of heating time (Fig. 6A) and temperature (Fig. 6B) was investigated. Note that for a heat treatment time of 15 s at 72 °C the expected reduction is 7.8 $\log_{10}$. It can be seen in Fig. 6A and 6B that due to the variability in the *D*-value some curvature is visible and the effects are not fully linear.

The effect of the standard deviation of the $\log_{10}D_{72}$-value is shown in Fig. 6C. When the standard deviation is very small the reduction goes to the expected mean reduction of 33 $\log_{10}$. For very high values the reduction becomes very small, since there are cells with a very high heat resistance, not being inactivated at all.

The results also depend on the assumed *z*-value (Fig. 6D). Aryani et al. (2015) determined the *D*-values of the 20 *L. monocytogenes* strains at 55 °C, 60 °C and 65 °C, and for the most heat resistant strain also at 70 °C, and we estimated the D_{72}-values based on extrapolation to 72 °C because inactivation at 72 °C goes too fast to be experimentally determined.

The effect of temperature is very large, and therefore the *y*-axis in Fig. 6B had to be $\log_{10}$-transformed. Clearly, the temperature is the

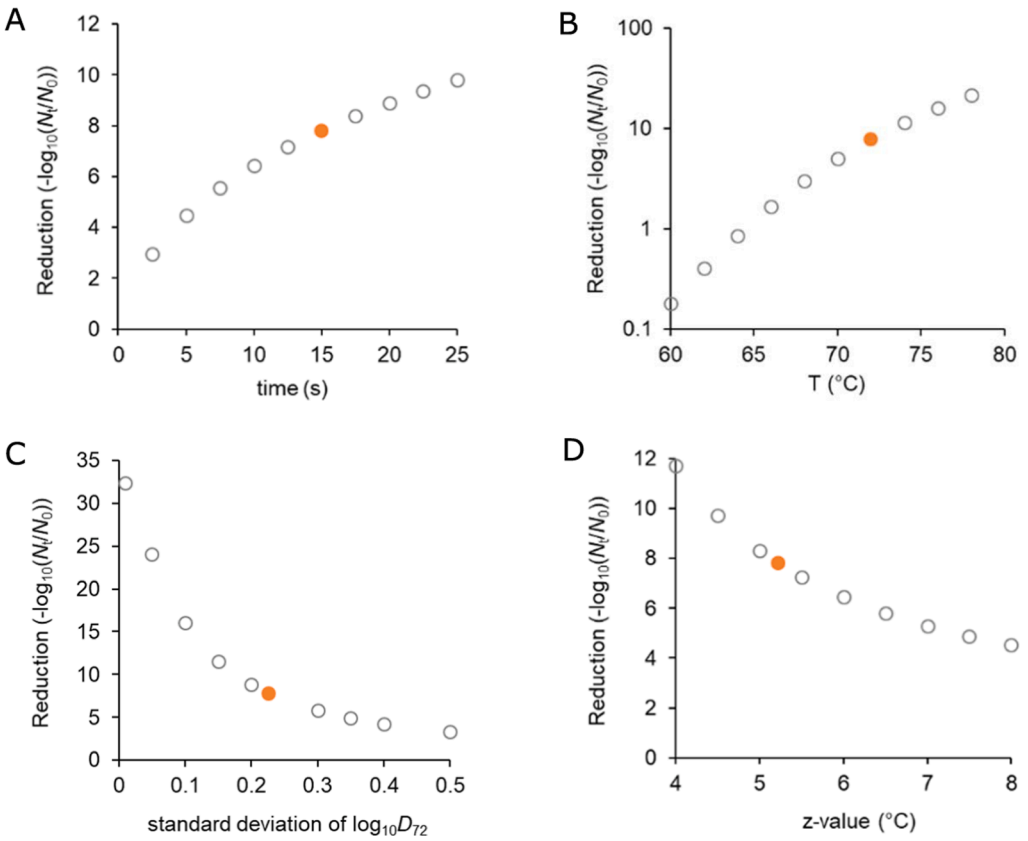

Fig. 6. Sensitivity analysis of impact of various variables on the achieved overall reduction of cells ($-\log_{10}(N_t/N_0)$) when heat treated and taking into account the variability in decimal reduction time with mean $\log_{10}D_{72}$ – 0.343 $\log_{10}$(s) and standard deviation 0.226 $\log_{10}$(s), calculated using the numerical approach. Effect of heating time on the reduction for a heat treatment at 72 °C (panel A); effect of temperature on the reduction for a heat treatment for 15 s (panel B, note that *y*-axis scaling is logarithmic); effect of the standard deviation of the $\log_{10}D_{72}$ on the reduction for a heat treatment at 72 °C for 15 s (panel C); effect of the *z*-value on the reduction for a heat treatment at 72 °C for 15 s. In orange the reduction for the reference condition with the standard deviation of the $\log_{10}D_{72}$ 0.226 $\log_{10}$(s), heat treatment at 72 °C for 15 s, and *z*-value of 5.22 °C. (For interpretation of the references to color in this figure legend, the reader is referred to the web version of this article.)

factor that has the largest effect on control – only slight temperature deviations have a huge impact on achieved reduction, and tight temperature control is crucial.

3.4. Efficacy of UHT processing on inactivation of Geobacillus stearothermophilus spores

As a second example to illustrate how strain variability affects the achieved microbial reduction, we used the *D*-values of spores of 18 strains of *Geobacillus stearothermophilus*, determined at 125 °C and 130 °C (Wells-Bennik et al., 2019). Based on these 18 strains the strain variability in $\log_{10}D$-values was determined and estimation of the *D*-values at different temperatures was done assuming a *z*-value of 11.1 °C (Wells-Bennik et al., 2019). The $\log_{10}$ inactivation was determined for the average $\log_{10}D$-value based on the 18 strains and on the 97.5th percentile using a numeric approach, and also using the Monte Carlo approach (Table 2).

When calculating the overall reduction taken into account the strain variability (i.e. $R_{numeric}$), the achieved reduction is about 3 $\log_{10}$ lower than when using the average $\log_{10}D$-value (i.e. R_{avgD}) when the heat treatment is performed at 120 °C for 1200 s, and the difference between these values becomes higher when the heat treatment becomes more severe. However, the inactivation of strains at the 97.5th percentile ($R_{97.5}$) show even lower reductions. In these simulations (both numeric and MC) the inactivation determined taking the whole distribution into account corresponds with the *D*-value at around the 90-95th percentile. The differences between $R_{numeric}$ and R_{avgD} are less extreme than for *Listeria* presented above. This can be explained by two reasons. Firstly, the standard deviation for *Geobacillus* is lower (0.171 $\log_{10}$(s)versus 0.226 $\log_{10}$(s) for *Geobacillus* and *Listeria*, respectively). We showed that especially the right-hand tail of the distribution of the $\log_{10}D$-values determines the overall achieved reduction and when the standard deviation is lower, then also the prevalence of extremely highly heat resistant strains is lower. And, secondly, the targeted reduction in this second example is lower, since *Geobacillus* is a spoiler and not a pathogen. When for *Geobacillus* higher reductions are targeted (see for example heat treatment for 20 s at 145 °C), then also the more extreme parts of the $\log_{10}D$-value distribution become more relevant and the

Table 2
D-value (s) and reduction -$\log_{10}(N_t/N_0)$ of *Geobacillus stearothermophilus* spores for various time *t* (s)-temperature *T* (°C) combinations determined with the average $\log_{10}D$-value ($\log_{10}$(s)), the 97.5th upper percentile of the $\log_{10}D$-value distribution and the whole distribution using the numeric approach, and the Monte Carlo (MC) approach.

T (°C)	*t* (s)	$D_{average}$ (s)	R_{avgD} ($-\log_{10}(N_t/N_0)$)	$D_{97.5\ upper}$ (s)	$R_{97.5}$ ($-\log_{10}(N_t/N_0)$)	$R_{numeric}$ ($-\log_{10}(N_t/N_0)$)	R_{MC} ($-\log_{10}(N_t/N_0)$)
120	1200	178	6.76	390	3.07	4.02	4.03
121.1	1000	141	7.07	311	3.22	4.14	4.15
125	500	63.1	7.92	139	3.60	4.46	4.46
130	180	22.4	8.02	49.4	3.65	4.50	4.50
135	60	7.98	7.52	17.6	3.42	4.31	4.32
140	20	2.84	7.05	6.24	3.20	4.13	4.14
145	10	1.01	9.91	2.22	4.51	5.15	5.16
145	20	1.01	19.8	2.22	9.01	7.77	7.76

For the $\log_{10}D$ ($\log_{10}$(s)) at 140 °C a Normal distribution (mean 0.00385, standard deviation 0.171) and a *z*-value of 11.1 °C was used.

differences between $R_{numeric}$ and R_{avgD} is large again and the $R_{numeric}$ gives a lower reduction than the 97.5th percentile of the $\log_{10}D$-values. The values for the numeric approach and the Monte Carlo calculation are virtually equal, showing again that both approaches result in equal outcomes and can both be used to calculate the overall reduction.

4. Discussion

Food processors are producing very large volumes of foods, and then looking at efficacy of critical control steps at a large scale is of importance. As discussed in this paper, a factor that is very relevant for the efficacy of an inactivation treatment is strain-to-strain variation. However, this is a parameter inherent to microorganisms and cannot be controlled by the producer. Additionally, the physiological state of the organism (related to its history) can have a large impact (Den Besten et al., 2017; Richter et al., 2010; Smelt & Brul, 2014; Li & Gänzle, 2016), and this latter factor cannot be easily controlled either. Instead, producers must manipulate other factors that also influence the level of inactivation during a heat treatment. For instance, process characteristics such as temperature and duration, or properties of the product like water activity or pH. Additional matrix effects, like the fat content, might also be relevant (Verheyen et al., 2019a, Verheyen et al., 2019b, Verheyen et al., 2020).

In this analysis it is assumed that inactivation is log-linear, thus, not taking account of a curvature. This choice was made since other effects on inactivation, like T, matrix and strain variability are much more affecting the inactivation efficacy for the microorganisms analyzed (Aryani et al., 2016; Van Asselt & Zwietering, 2006; Wells-Bennik et al., 2019). Including a curvature parameter, for example using the Weibull model (Van Boekel, 2002), increases the complexity of the calculations and is hard to generalize for other microorganisms and conditions, due to the large variability of this value between different conditions.

Both the numeric-kinetic approach and the Monte Carlo approach give valuable insight and can be done in parallel. These approaches highlighted the relevance of the tails of the $\log_{10}D$-value distribution, and the effect of introduced asymmetry when calculating the reduction. The kinetic approach shows in which part of the distributions most of the survivors are found (Fig. 1). The stochastic approach shows actual iterations of resulting survivors (Fig. 5). In the analysis performed in this study, the kinetic approach and the Monte Carlo approach gave similar outcomes, which is not surprising, but gives reassurance that the calculations are correctly implemented and that the outcomes are stable (sufficient number of iterations). The assessment of food safety is a complex topic, where calculation or methodological errors are possible (Zwietering, 2009). It is, thus, sensible to verify calculations, ideally applying a different approach, as done in this paper. Due to the skewness and asymmetry of the distributions and the application of non-linear mathematical transformations, it is relevant to investigate factors on different scales as we did with $\log_{10}D$, reduction, and number of survivors (Tables 1 and 2). The average on one scale will not be at the same place as the average on the other scale (see Appendix B). For average consumer exposure, the arithmetic number of survivors is most relevant.

In this study we showed that a kinetic approach and a stochastic approach can be applied to determine the effect of strain variability on achieved microbial reduction. For the kinetic approach an integral equation (Eq. (5)) has to be solved numerically, making use of many small integration steps. For the numeric approach the integration steps need to be small enough to get a stable outcome, while for the stochastic approach the number of iterations needs to be large enough to get a stable outcome. Therefore, the truncation error is a source of uncertainty that impacts the outcome of the investigation. Its relevance should be investigated by decreasing the integration step-size and by increasing the number of iterations to check if the variable of interest converges within a reasonable tolerance. In both approaches, due to the relevance of the right-hand tail, many iteration (Monte Carlo) and many small time steps (numeric approach) were needed to come to stable outcomes. Since both analyses give insight and also give a confirmation of the magnitude of the effect, it is advised to more often do both analyses instead of only one.

It should be realized that the prevalence of the extreme D-values based on the normal distribution determined with 20 strains, might be not fully accurate and representative. The estimation of the standard deviation based on many more strains might slightly differ and, as presented in this paper, small differences in standard deviation significantly affect the overall reduction. Furthermore, the distribution as quantified for the 20 strains will not be fully representative for the variability that will be found in practice. So, the 'real' distribution of $\log_{10}D$-values can be different from the distribution based on the specific selection of 20 strains. Also, some strains can be more common in a specific food commodity and this also determines the expected microbial variability in the food of interest (Painset et al., 2019). On the other hand, a recent review comparing the strain variabilities among different species, including sporeforming and vegetative cells, concluded that the order of magnitude among species is rather comparable (Den Besten et al., 2018), though the exact values really differ.

It can be concluded from this paper that including the effect of strain-to-strain variability in heat resistance has a large impact on the obtained reduction, especially for harsh processes.

CRediT authorship contribution statement

Marcel H. Zwietering: Conceptualization, Methodology, Software, Visualization. **Alberto Garre:** Conceptualization, Methodology, Software, Visualization. **Heidy M.W. den Besten:** Conceptualization, Methodology, Software, Visualization.

Acknowledgements

Olivier Cerf is acknowledged for bringing up the idea to determine the inactivation by Monte Carlo analysis. Alberto Garre was supported by a postdoctoral granted by the Fundación Seneca (20900/PD/18) and by the European Union's Horizon 2020 research and innovation programme under the Marie Sklodowska-Curie Individual Fellowship grant No 844423 (FANTASTICAL).

Appendix A. Supplementary material

Supplementary data to this article can be found online at https://doi.org/10.1016/j.foodres.2020.109973.

References

Aryani, D. C., Den Besten, H. M. W., Hazeleger, W. C., & Zwietering, M. H. (2015). Quantifying variability on thermal resistance of *Listeria monocytogenes*. *International Journal of Food Microbiology, 193*, 130–138. https://doi.org/10.1016/j.ijfoodmicro.2014.10.021.

Aryani, D. C., Zwietering, M. H., & Den Besten, H. M. W. (2016). The effect of different matrices on the growth kinetics and heat resistance of *Listeria monocytogenes* and *Lactobacillus plantarum*. *International Journal of Food Microbiology, 238*, 326–337. https://doi.org/10.1016/j.ijfoodmicro.2016.09.012.

Balsa-Canto, E., Alonso, A. A., & Banga, J. R. (2008). Computational procedures for optimal experimental design in biological systems. *IET Systems Biology, 2*(4), 163–172. https://doi.org/10.1049/iet-syb:20070069.

Bean, D., Bourdichon, F., Bresnahan, D., Davies, A., Geeraerd, A., Jackson, T., Membre, J. M., Pourkomailian, B., Richardson, P., Stringer, M., Uyttendaele, M., & Zwietering, M. (2012). Risk assessment approaches to setting thermal processes in food manufacture. ILSI Europe Report Series, ILSI, Brussels, 40p. https://ilsi.eu/wp-content/uploads/sites/3/2016/06/Thermal-processing.pdf.

Den Besten, H. M. W., Wells-Bennik, M. H. J., & Zwietering, M. H. (2018). Natural diversity in heat resistance of bacteria and bacterial spores: Impact on food safety and quality. *Annual Review of Food Science and Technology, 9*, 383–410. https://doi.org/10.1146/annurev-food-030117-012808.

Den Besten, H. M. W., Aryani, D. C., Metselaar, K. I., & Zwietering, M. H. (2017). Microbial variability in growth and heat resistance of a pathogen and a spoiler: All variabilities are equal but some are more equal than others. *International Journal of Food Microbiology, 240*, 24–31. https://doi.org/10.1016/j.ijfoodmicro.2016.04.025.

ICMSF. (2018). *Microorganisms in Foods 7: Microbiological Testing in Food Safety Management* (Second Edition). Switzerland: Springer International Publishing AG.

Li, H., & Gänzle, M. (2016). Some like it hot: Heat resistance of *Escherichia coli* in food. *Frontiers in Microbiology, 7*, 1763. https://doi.org/10.3389/fmicb.2016.01763.

McMeekin, T. A., Olley, J., Ratkowsky, D. A., & Ross, T. (2002). Predictive microbiology: Towards the interface and beyond. *International Journal of Food Microbiology, 73* (2–3), 395–407. https://doi.org/10.1016/S0168-1605(01)00663-8.

Painset, A., Björkman, J. T., Kiil, K., Guillier, L., Mariet, J.-F., Félix, B., … Dallman, T. J. (2019). LiSEQ – whole-genome sequencing of a cross-sectional survey of *Listeria monocytogenes* in ready-to-eat foods and human clinical cases in Europe. *Microbial Genomics, 5*(2), Article e000257. https://doi.org/10.1099/mgen.0.000257.

Richter, K., Haslbeck, M., & Buchner, J. (2010). The heat shock response: Life on the verge of death. *Molecular Cell, 40*(2), 253–266. https://doi.org/10.1016/j.molcel.2010.10.006.

Smelt, J. P. P. M., & Brul, S. (2014). Thermal inactivation of microorganisms. *Critical Reviews in Food Science and Nutrition, 54*(10), 1371–1385. https://doi.org/10.1080/10408398.2011.637645.

Van Asselt, E. D., & Zwietering, M. H. (2006). A systematic approach to determine global thermal inactivation parameters for various food pathogens. *International Journal of Food Microbiology, 107*, 73–82. https://doi.org/10.1016/j.ijfoodmicro.2005.08.014.

Van Boekel, M. A. J. S. (2002). On the use of the Weibull model to describe thermal inactivation of microbial vegetative cells. *International Journal of Food Microbiology, 74*(1–2), 139–159. https://doi.org/10.1016/S0168-1605(01)00742-5.

Verheyen, D., Baka, M., Akkermans, S., Skåra, T., & Van Impe, J. F. (2019). Effect of microstructure and initial cell conditions on thermal inactivation kinetics and sublethal injury of *Listeria monocytogenes* in fish-based food model systems. *Food Microbiology, 84*, Article 103267. https://doi.org/10.1016/j.fm.2019.103267.

Verheyen, D., Xu, X. M., Govaert, M., Baka, M., Skåra, T., & Van Impe, J. F. (2019). Food Microstructure and fat content affect growth morphology, growth kinetics, and preferred phase for cell growth of *Listeria monocytogenes* in fish-based model systems. *Applied and Environmental Microbiology, 85*(16), e00707–e00719. https://doi.org/10.1128/AEM.00707-19.

Verheyen, D., Bolívar, A., Pérez-Rodríguez, F., Baka, M., Skåra, T., & Van Impe, J. F. (2020). Isolating the effect of fat content on *Listeria monocytogenes* growth dynamics in fish-based emulsion and gelled emulsion systems. *Food Control, 108*, Article 106874. https://doi.org/10.1016/j.foodcont.2019.106874.

Wells-Bennik, M. H. J., Janssen, P. W. M., Klaus, V., Yang, C., Zwietering, M. H., & Den Besten, H. M. W. (2019). Heat resistance of spores of 18 strains of *Geobacillus stearothermophilus* and impact of culturing conditions. *International Journal of Food Microbiology, 291*, 161–172. https://doi.org/10.1016/j.ijfoodmicro.2018.11.005.

Zwietering, M. H. (2009). Quantitative risk assessment: Is more complex always better? Simple is not stupid and complex is not always more correct. *International Journal of Food Microbiology, 134*, 57–62. https://doi.org/10.1016/j.ijfoodmicro.2008.12.025.

Zwietering, M. H. (2015). Risk assessment and risk management for safe foods: Assessment needs inclusion of variability and uncertainty, management needs discrete decisions. *International Journal of Food Microbiology, 213*, 118–123. https://doi.org/10.1016/j.ijfoodmicro.2015.03.032.